Journal of Chromatography A 1741 (2025) 465614

Contents lists available at ScienceDirect

Journal of Chromatography A

journal homepage: www.elsevier.com/locate/chroma

Methylcellulose enhances resolution in gravitational field-flow fractionation: Going beyond viscosity

R. Danusso [a,b,*], G. Iamoni [a,c], A. Moles [a,c], G. Casagrande [c], L. Possenti [d], I. Cetin [a], D. Lattuada [a]

[a] Department "Area Materno-Infantile" Fondazione IRCCS Ca' Granda Ospedale Maggiore Policlinico, Milan Italy
[b] School of Medicine and Surgery, University of Milano-Bicocca, Milan Italy
[c] Department of Chemistry, Materials and Chemical Engineering "Giulio Natta", Politecnico di Milano, Milan Italy
[d] Data Science Unit, Fondazione IRCCS Istituto Nazionale Tumori, Milan Italy

ARTICLE INFO

Keywords:
Gravitational Field-Flow Fractionation (GrFFF)
Viscosity
Polystyrene-based (PS) microbeads
Resolution
Methyl-Cellulose

ABSTRACT

Gravitational Field-Flow Fractionation (GrFFF) is an elution-based method designed for the separation of particles ranging from a few micrometers up to approximately 100 μm in diameter. Separation occurs over time, with particles being fractionated based on size and other physico-chemical properties. GrFFF takes advantage of gravitational forces acting perpendicularly to a laminar flow in a thin channel. The fluid exhibits a parabolic velocity profile, with the maximum velocity at the center of the channel and zero velocity at the walls. The exit time of particles depends on their equilibrium position relative to the bottom wall. In hyperlayer mode, larger particles elute faster than smaller ones due to their higher velocities within the channel.

This study investigated the effect of adding methylcellulose (MC) to the carrier fluid on the elution behavior - specifically, peak time (t_{peak}) and resolution (R) - of polystyrene-based (PS) microparticles with sizes of 7, 8, and 10 μm. The results demonstrated that MC not only increases the viscosity of the carrier fluid but also exerts a secondary, predominant effect that improves resolution (R), thereby enhancing the separation of particle populations. This was confirmed by comparing the use of water as the carrier fluid at two different temperatures: 14 °C (high viscosity) and 28 °C (low viscosity). While increasing viscosity by lowering temperature only led to modest reduction in elution time of the fractograms, the addition of MC had a size-dependent effect on the microparticles, significantly improving R without changing other experimental parameters. This suggests the presence of additional phenomena contributing to the improved separation.

In conclusion, the addition of MC to the carrier fluid increases the resolving power of GrFFF, enabling the separation of PS microbeads with a size difference of up to 2 μm. This advancement pushes the boundaries of GrFFF and opens up potential new applications. These studies, conducted on PS microbeads, provide a preliminary basis for future work on cells, which have similar density and size. This could pave the way for improved cell separation in diagnostic applications.

1. Introduction

Field-Flow Fractionation (FFF) is an elution-based technique for size separation. It employs external fields acting perpendicularly to the direction of the fluid flowing within a channel, separating particles by size, ranging from nanometers up to 100 μm micrometers. It was introduced in the 1960s [1] and encompasses various methodologies employing external field applications to cater to diverse sample characteristics [2]. It differs from chromatography as FFF only has one phase, specifically the mobile phase. The main advantages of FFF are simple instrumentation, convenient operation, and low operating costs.

Among the variants of FFF, the Gravitational Field-Flow Fractionation (GrFFF) employs Earth's gravity as a field force pushing particles toward the bottom of the channel.

GrFFF is suitable for the physiological separation of cells without tags due to the gentle nature of the fractionation process [3]. It is also widely used for the separation of polymeric beads [4], bacteria [5], and yeasts [6].

* Corresponding author at: Foundation IRCCS Cà Granda Ospedale Maggiore Policlinico, Department "Area Materno-Infantile", Milan, Italy.
E-mail address: roberta.danusso@policlinico.mi.it (R. Danusso).

https://doi.org/10.1016/j.chroma.2024.465614
Received 16 December 2024; Accepted 18 December 2024
Available online 20 December 2024

The separation occurs at the bottom of the channel due to gravity- and drag-driven forces. For this reason, particles are usually sedimented to the bottom of the channel before the separation starts. The flow is typically laminar, as commonly happens in microfluidic channels, resulting in the classical parabolic profile with the maximum velocity at the center of the channel and zero velocity at the walls.

When the carrier fluid flows, the hydrodynamic lift force (HLF) pushes the particles away from the bottom wall, acting in the opposite direction to gravity. When this force balances the gravitational force, particles reach their vertical equilibrium position. Such an equilibrium position determines particle velocity, affects elution time, and leads to particle separation.

Various physical and chemical factors can affect the two forces: carrier properties (viscosity, density, and ionic strength), channel geometry (height, length, and width), and carrier fluid flow rate, which directly influences the velocity of particles in the channel [7].

The ultimate objective of this research is to develop a method to separate blood cells under physiological conditions. These cells possess density and dimensions comparable to polystyrene (PS) microbeads [8], which are used as model particles in this study. The focus is to optimize the separation process by investigating the influence of methylcellulose (MC) on PS microbead separation. The efficacy is quantitatively evaluated in terms of Resolution (R), the system's ability to separate particles of different sizes.

2. Theory

The GrFFF process results from a combination of gravitational force, lift forces, and flow-induced drag [4].

The **Gravitational Force** acting on a particle is defined as in Eq. (1):

$$F_G = \frac{4}{3}\pi r^3 \Delta\rho g \cos\theta \tag{1}$$

where r is the particle radius, $\Delta\rho$ is the difference between particle and carrier density, g is the gravitational acceleration, and θ is the channel inclination angle (θ = 0, cosθ = 1, in our application).

On the same particle, we define the **Hydrodynamic Lift Force** as in Eq. (2) [7]:

$$F_L = C\,6\frac{\mu\bar{v}}{h\delta}r^3 \tag{2}$$

where C is an empirical dimensionless coefficient (it depends on many different experimental factors, such as h), μ is the viscosity, $\bar{v}$ is the fluid mean velocity, h is the height of the channel, δ is the equilibrium distance from the bottom wall to the particle surface, and r is the particle radius.

To obtain the equilibrium distance, we solve the force balance as a function of δ, yielding to Eq. (3):

$$\delta_{eq} = \frac{9}{2}\frac{C}{\pi g}\frac{\mu\bar{v}}{h\Delta\rho\cos\theta} \tag{3}$$

The equilibrium distance depends proportionally on the fluid viscosity (μ), and mean velocity ($\bar{v}$). On the other hand, it is inversely proportional to the channel height (h), orientation ($\cos\theta$), and the difference between the particle and fluid densities ($\Delta\rho$).

It is interesting to note that the equilibrium distance is independent of the particle radius. This means that all particles have the same equilibrium distance. However, the radius comes back into play when computing the particle velocity, which is evaluated at the particle center (x_{eq}, *equilibrium position,* i.e. *the distance between the particle center and the bottom wall)* as described in Eq. (4):

$$x_{eq} = \delta_{eq} + r \tag{4}$$

The fluid velocity profile in the channel follows Eq. (5):

$$v(x) = 6\bar{v}\frac{x}{h}\left(1 - \frac{x}{h}\right) \tag{5}$$

where x is the vertical coordinate (bottom wall: $x = 0$; top wall: $x = h$).

The particle assumes the fluid velocity (described in Eq. (6)) in position x_{eq}, scaled by a retardation factor, accounting for drag-induced phenomena:

$$v_p(x_{eq}) = f\left(\frac{\delta}{r}\right)v(x_{eq}) \tag{6}$$

where the retardation factor is defined in Eq. (7) [9]:

$$f\left(\frac{\delta}{r}\right) = \begin{cases} \dfrac{1}{0.66 - 0.2693\ln(\delta/r)}, & \dfrac{\delta}{r} < 0.005 \\ 1 - \dfrac{5}{16}\left(\dfrac{r}{x}\right)^3, & \dfrac{\delta}{r} \geq 0.5 \end{cases} \tag{7}$$

All the equations are gathered in Fig. 1.

3. Materials and methods

Carrier fluids. The carrier fluid solutions employed were:

- H_2O for injectable preparations (Fresenius Kabi, Bad Homburg vor Der Höhe, Germany).
- H_2O for injectable preparations + 0.2 % methylcellulose (MC), obtained by dissolving 1 g of methylcellulose (Merck-KJaA, Darmstadt, Germany) in 0.5 L of H_2O for injectable preparations aided by a magnetic mixer.

Polystyrene Latex Beads. The samples were polystyrene (PS) latex beads obtained from Merck-KJaA (Darmstadt, Germany), with defined nominal diameters and standard deviations (B7: 7 ± 0.11 μm; B8 8 ± 0.11 μm; B10 10 ± 0.14 μm).

PS microbeads were employed as a homogeneous population or a 50–50 mixture of two populations (BMIX). Each injected sample (homogeneous or mixed) contained 10^5 particles resuspended in deionized water (Fresenius Kabi, Bad Homburg vor der Höhe, Germany) with a final volume of 30 μL.

Gravitational FFF: apparatus and tests. The GrFFF channel used was assembled in our laboratory. It was 200 μm high, 2 cm wide, and 30 cm long. The device was made of two slabs of different materials: the bottom one is polyvinyl chloride (PVC), while the top one is polycarbonate (PC). Between these two slabs, a 200 μm carved Mylar film sheet defines the channel's height. A schematic representation of GrFFF device is in Figure S1.

In all experiments, the PS microbead samples were injected directly into the channel using a 50 μL syringe (Hamilton Co., Reno, NV, USA). The flow was halted for 4 min to let the particles settle at the bottom of the channel.

Then, the carrier solution was pumped by a peristaltic pump Mini Plus 3 (Gilson, Middleton, WI, USA). The elution of the sample was monitored by a UV/VIS spectrophotometer model V-530 (Jasco, Tokyo, Japan) at the operating wavelength of 600 nm to acquire the tracing of the absorbance over time during each experiment. All the connecting tubes were made of PEEK tubes (Grace Davison Discovery Science, Columbia, MD, USA).

All the experiments, along with their corresponding numerosity, are summarized in Supplementary Table S1.

Viscosity assessment Two different temperatures, 'COLD' (T_{mean} = 14 °C) and 'HOT' (T_{mean} = 28 °C), and two different compositions (with 0.2 % MC and without MC), resulting in four conditions, were analyzed to evaluate the viscosity of the carrier fluid solution. Viscosity was assessed using a routine viscometer series 100 (Cannon Fenske, State College, PA, United States).

Viscosity was computed as $\mu = C \cdot t \cdot \rho$, where C = 0.01588 cP($cm^3$/

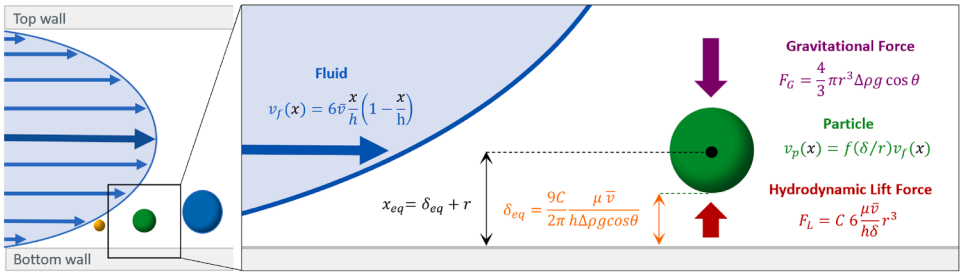

Fig. 1. Side view of the channel and physics behind GrFFF.

g)/s is the viscometer constant and $\rho = 1.0$ g/cm^3 is the density of pure water. Every measurement was repeated three times, and the values were averaged.

Fractograms post-processing After the acquisition, the fractograms were filtered through a bandpass filter (order 10, window 0.02–0.12 Hz, sample rate 20 Hz; coded using MATLAB version R2023b, MathWorks Inc., Natick, MA, USA). Subsequently, we extracted parameters for each experiment: peak time t_{peak}, Δt, and σ, as represented in Fig. 2. The peak time is defined as the time coordinate corresponding to the local maximum of the absorbance of the fractograms, Δt is the difference between peak times if multiple peaks are present, σ is the half-width of a single peak, under the assumption of Gaussianity. The resolution (R) parameter is computed in Eq. (8), taken from [10]:

$$R = \frac{\Delta t}{\sigma_1 + \sigma_2} \tag{8}$$

Resolution refers to the system's ability to distinguish and separate two distinct populations in an analysis. When only a single peak is observed, despite loading two distinct populations into the channel, the resolution is defined as $R = 0$, indicating no separation. As the degree of separation improves, the resolution increases accordingly. A resolution value of $R \geq 1.5$ signifies complete separation, where the two populations are fully resolved from one another.

Microscopic dimensional analysis During the GrFFF experiments, fractions corresponding to the peaks were collected on the Makler chamber slides, and a dimensional analysis was performed using ImageJ software (ImageJ 1.52p, Wayne Rasband, National Institute of Health, USA) to verify the diameter of the eluted particles.

Statistical analysis. The analysis was performed using "Statistical Package for Social Science 29.0" (SPSS Inc., Chicago, Illinois). The difference between groups was compared using the non-parametric Mann-Whitney U test. Peak times are expressed as median and first and third quartile, and are represented in boxplot graphs. P-values lower than 0.05 have been considered statistically significant.

4. Results

4.1. Viscosity and pH assessment

The viscosities of the carrier fluid in the different experimental conditions are listed in Table 1. The results were reported as the mean of three tests.

The viscosity is always lower in the 'HOT' condition, and the presence of 0.2 % MC increases the viscosity measured. The pH value of water for injectable preparations used in the experiments presented is 4.88 ± 0.07 for cold water and 5.36 ± 0.09 for hot water. These values increase to 6.21 ± 0.06 and become stable regardless of temperature in the presence of 0.2 % methylcellulose.

4.2. Effect of methylcellulose (MC)

Firstly, the effect of the addiction of MC to the carrier fluid at 28 °C was evaluated in GrFFF experiments conducted on PS microbead mixtures. The sample consists of PS microbeads of 7 and 10 micrometers (Fig. 3A), and subsequently 8 and 10 micrometers (Fig. 3B). When using only water as a carrier, the spectra show a single peak (t_{peak} = 35.3

Table 1
Results of viscosity and pH assessment.

	H_2O			H_2O + 0.2 % MC		
	t [s]	μ [cP]	pH	t [s]	μ [cP]	pH
HOT (28 °C)	58.1 ± 0.6	0.92 ± 0.01	5.36 ± 0.09	81.8 ± 0.7	1.30 ± 0.01	6.21 ± 0.06
COLD (14 °C)	67.6 ± 0.6	1.07 ± 0.01	4.88 ± 0.07	90.8 ± 2.6	1.44 ± 0.04	6.21 ± 0.04

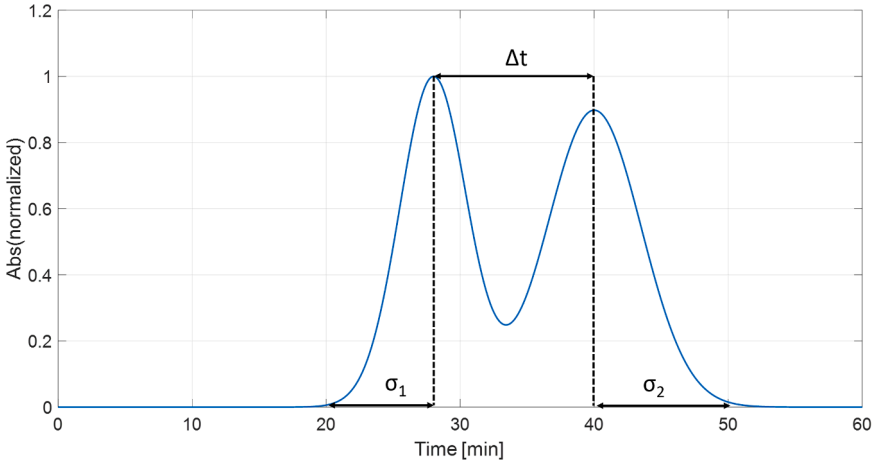

Fig. 2. Graphical representation of the parameters extracted from each fractogram.

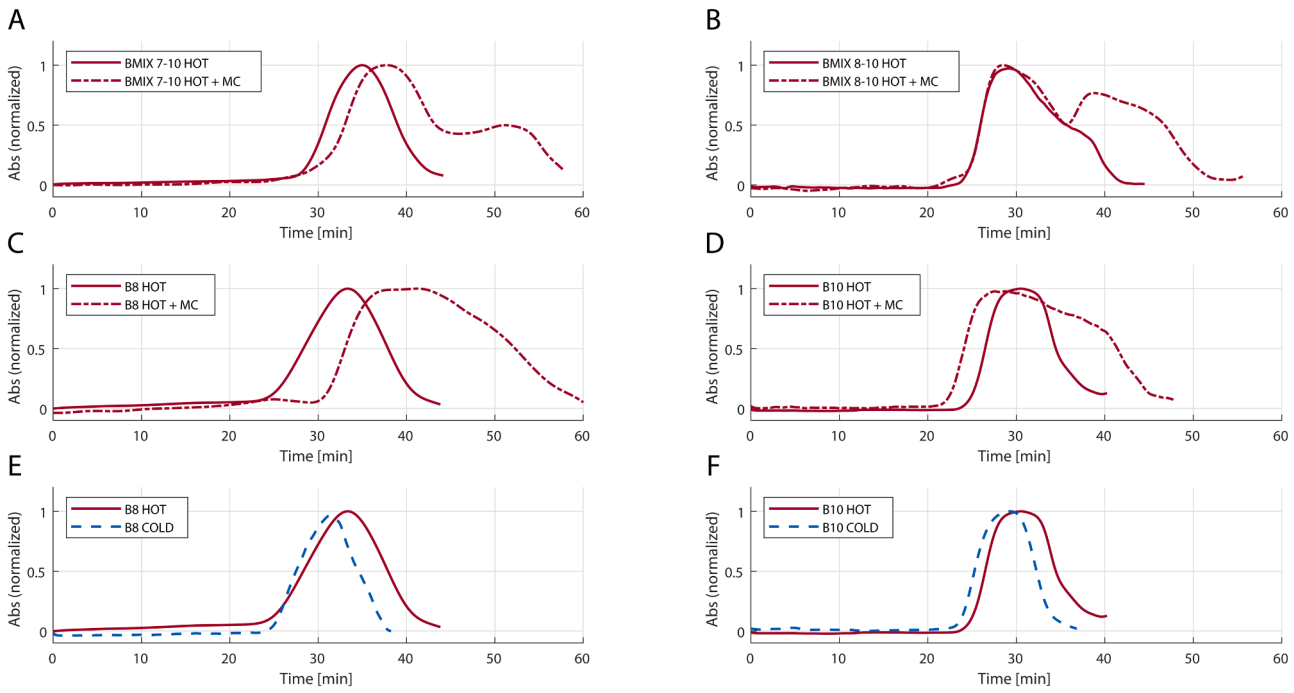

Fig. 3. Absorbance over time graphs of GrFFF separation of **3A)** PS microbeads mix (7 μm and 10 μm) with HOT water (red continuous line) and HOT water + 0.2 % MC (red dash-dot line), $Q = 270$ μL/min; **3B)** PS microbeads mix (8 μm and 10 μm) with HOT water (red continuous line) and HOT water + 0.2 % MC (red dash-dot line) $Q = 320$ μL/min; **3C)** PS microbeads 8 μm with HOT water (red continuous line) and HOT water + 0.2 % MC (red dash-dot line), $Q = 320$ μL/min; **3D)** PS microbeads 10 μm with HOT water (red continuous line) and HOT water + 0.2 % MC (red dash-dot line) $Q = 320$ μL/min; **3E)** PS microbeads 8 μm with HOT water (red continuous line) and COLD water (blue dashed line), $Q = 320$ μL/min; **3F)** PS microbeads 10 μm with HOT water (red continuous line) and COLD water (blue dashed line), $Q = 320$ μL/min.

(34.0–35.3) min for B7–10 and $t_{peak} = 28.4$ (27.4–29.4) min for B8–10). When MC is added, a second peak appears mainly populated by smaller-sized particles (1° $t_{peak} = 37.7$ (37.6–37.7) min, 2° $t_{peak} = 51.3$ (51.0–51.6) min, $\Delta t = 13.6$ min for B7–10 and 1° $t_{peak} = 28.6$ (28.3–28.9) min, 2° $t_{peak} = 39.6$ (39.4–39.8) min, $\Delta t = 11$ min for B8–10).

The sample composition of the two peaks, collected after the experiments, was verified *via* dimensional analysis, confirming the successful separation as shown in Supplementary Figure S2. Therefore, in both cases, adding MC causes the spectra to show two peaks, consisting mainly of the two populations of PS microbeads. While the t_{peak} for B10 does not statistically change, the t_{peak} for B7 and B8 increases with statistical significance ($p = 0.001$ for B7 and $p = 0.046$ for B8), determining an improvement of R from 0 (water) to $R = 0.85$ for BMIX 7–10 and $R = 0.61$ for BMIX 8–10, when MC is added.

To assess the effects of the addition of MC to the carrier fluid based on the PS microbead dimensions, experiments with homogeneous populations of B8 and B10 were carried out. The spectra show that the presence of MC for B8 causes a delay in peak time (from $t_{peak} = 32.2$ (31.3–32.4) min without MC to $t_{peak} = 41.3$ (41.2–41.3) min with 0.2 % MC - Fig. 3C). Conversely, adding the MC for B10 causes a change in shape and a slight reduction of the peak time ($t_{peak} = 30.5$ (30.3–30.5) min without MC to $t_{peak} = 27.7$ (27.3–28.8) min with 0.2 % MC, Fig. 3D). The t_{peak} shift value exhibits statistical significance for both samples: $p = 0.014$ for B8 and $p = 0.046$ for B10.

The effect of increasing viscosity was also evaluated with experiments in COLD condition ($T = 14$ °C) compared to HOT condition. The temperature reduction (from 28 °C to 14 °C) determines an increase in viscosity, comparable with the one of the addition of MC, causing a reduction in peak time for both B8 and B10 (B8: from $t_{peak} = 32.3$ (32.0–32.9) min to $t_{peak} = 31.2$ (31.1–31.3) min; $p = 0.046$, Figure 3E; B10: from $t_{peak} = 30.5$ (30.3–30.5) min to $t_{peak} = 29.6$ (29.1–29.7) min; $p = 0.046$, Fig. 3F).

We then compare the four experimental conditions (COLD/HOT and no MC/MC) for the BMIX 7–10, gathered in Fig. 4.

First of all, a decrease in temperature leads to a statistically significant peak time reduction (COLD $t_{peak} = 33.8$ (33.4–34.2) min, HOT $t_{peak} = 35.3$ (34.0–35.3) min, $p = 0.043$). The addition of MC in the HOT case induces a statistically significant delay (HOT + MC 1° $t_{peak} = 37.7$ (37.6–37.7) min and HOT + MC 2° $t_{peak} = 51.3$ (51–51.6) min vs. HOT $t_{peak} = 35.3$ (34.0–35.3); $p = 0.007$ and $p = 0.001$, respectively). On the other hand, under COLD conditions, the delay is significant for the second peak solely (COLD + MC 1° $t_{peak} = 34.9$ (34.1–35.6) min and COLD + MC 2° $t_{peak} = 47.5$ (46.6–48.1) min vs. COLD $t_{peak} = 33.8$ (33.4–34.2) min; p not significant and $p = 0.001$ respectively).

When considering the two peaks obtained with MC, the temperature increase yields a significant delay in both cases (HOT + MC 1° $t_{peak} = 37.7$ (37.6–37.7) min, and COLD + MC 1° $t_{peak} = 34.9$ (34.1–35.6) min, $p = 0.043$; HOT + 2° MC $t_{peak} = 51.3$ (51–51.6) min, and COLD + MC 2° $t_{peak} = 47.5$ (46.6–48.1) min, $p = 0.019$). The entire set of data is summarized in Supplementary Table S2, and the results of further analysis are in Supplementary Table S3 and Supplementary Figure S3.

The values of R, in the experiments employing MC, are similar in both temperature conditions: $R = 0.85$ for HOT and $R = 0.86$ for COLD, as well as the absence of separation ($R = 0$) was observed without MC.

5. Discussion

To the best of our knowledge, this study represents the first investigation on the resolution enhancement in the presence of methylcellulose in Gravitational Field-Flow Fractionation, investigating beyond viscosity. The experiments have highlighted a different effect of the temperature variation (Fig. 3E-F) and the addition of methylcellulose (Fig. 3A-D), even if they both altered the viscosity of the suspension. The variation in viscosity occurring with a decrease in temperature causes the hydrodynamic lift force to increase, allowing particles to reach higher equilibrium positions and thus elute faster (see Theory section). This effect is global and implies a slight reduction of the peak time of the

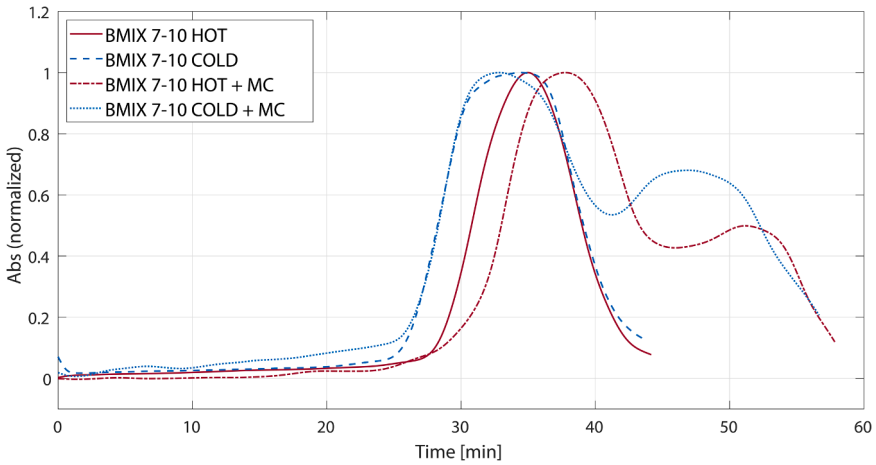

Fig. 4. Absorbance over time graphs of GrFFF separation of PS microbeads mix (7 μm and 10 μm) with HOT water (red continuous line), COLD water (blue dashed line), HOT + 0.2 % MC (red dash-dot line), and COLD + 0.2 % MC (blue dotted line), $Q = 270$ μL/min.

PS microbeads, which is always statistically significant. This reduction does not imply a variation in the resolution of the system because no additional peaks appear in BMIX experiments.

Conversely, MC addition improves resolution, given the delay effect dependent on the PS microbead's diameter. In our case, the presence of MC causes a delay in the elution of particles, whereas, in contrast to other studies, hydroxypropylmethylcellulose (HPMC) typically causes an earlier elution. This can be related to the use of HPMC instead of MC, to different channel manufacturing materials, and different channel geometries.

This size effect appears evident when considering both the mix and the homogeneous PS microbead populations. Indeed, the MC mainly affects smaller particles, inducing a delay more evident in 7 and 8 μm particles (Figs. 3–4). The peak corresponding to the 10 μm PS microbeads occasionally exhibits either a modest delay or a slight advance, accompanied by a noticeable change in the spectral shape.

We further tested the validity of our results with similar carrier solutions adding a surfactant (SDS) and a bactericide (Sodium azide), since they are often included in the carrier fluid. Our results (not shown here) are similar to those shown in the literature [4]. When the ionic strength increased following the addition of SDS and sodium azide, a modest delay in peak time was observed. This can be explained coherently by a reduction of the repulsive forces in the near-wall region. Anyway, since the final application of these method is aimed at cell separation, we did not consider them as they are affecting cell viability. Further insights on these additives can be found in literature [4], but we suggest a careful comparison considering the different working conditions (e.g., particle sizes, velocity of the carrier fluid, manufacturing materials of the channel, additive for the carrier fluid). Particularly, we remark the peculiarity of this work in analyzing particles with a narrow size range (7–10 μm).

Based on our results, a viscosity variation is not sufficient to explain the change in particle elution under the different conditions tested. Therefore, other phenomena should be considered. One of the possible phenomena regards alterations in the surface interactions between the PS microbeads and the fluid generated by electrostatic interactions. Both attractive and repulsive forces act in the near-wall region, especially influencing the retention of the smaller particles [11–13]. However, there are only a limited number of studies focused on investigating and quantifying the effects of these factors. The PS microbead's superficial charge supports such consideration. This charge density is thought to be proportional to the particle's radius, which might explain these size-dependent effects [14–16]. Nonetheless, these kinds of forces are complex to model and quantify [8,17].

On the other hand, multiple studies also reported alterations of the electric properties of water by MC, yielding alterations of pH (confirmed by our data), permittivity, and the Debye layer of the flowing particles (namely, the distance over which the surface charges influence the distribution of the ions in the solution, modifying in turn the repulsion forces between charged particles) [18–21]. However, these effects have never been thoroughly investigated and mathematically quantified.

Finally, adding MC might lead to a non-Newtonian behavior of the fluid, as per [22–23]. Such a viscoelastic nature of the fluid possibly affects particle migration in channel flow. More specifically, particle migration towards the channel wall occurs in shear-thinning liquids, while in the elasticity-dominated regime, particles tend to focus along the centerline. However, in our specific case, the MC concentration (2 g/l) is not sufficient to reach the non-Newtonian conditions for the shear rate characterizing the channel (variable between 40 and 80 s^{-1}).

In summary, the resolution enhancement observed in the presence of MC is not explained by the simple change in viscosity but also involves ionic/electrostatic interactions, which are not fully explained to date.

6. Conclusion

In conclusion, besides increasing viscosity, the methylcellulose (MC) in the carrier fluid also exerts a potentially beneficial secondary effect on the resolution of Gravitational Field-Flow Fractionation (GrFFF) experiments. While the role of viscosity is well-established, the significant enhancement in separation efficiency observed with MC suggests the presence of additional factors, possibly related to ionic or electrostatic interactions, that are not yet fully understood. These effects warrant further investigation and characterization to fully exploit their potential and optimize GrFFF for more precise and efficient separations. Such efforts could lead to improved experimental outcomes, paving the way for improved cell separation in biomedical applications and broadening the applicability of this technique in both research and translational/clinical settings.

CRediT authorship contribution statement

R. Danusso: Data curation, Formal analysis, Investigation, Software, Writing – original draft, Writing – review & editing. **G. Iamoni:** Data curation, Formal analysis, Methodology, Software, Writing – original draft, Writing – review & editing. **A. Moles:** Data curation, Formal analysis, Investigation, Software, Writing – original draft, Writing – review & editing. **G. Casagrande:** Data curation, Formal analysis, Investigation, Software, Writing – original draft, Writing – review & editing. **L. Possenti:** Data curation, Formal analysis, Investigation, Software, Writing – original draft, Writing – review & editing. **I. Cetin:** Data

curation, Formal analysis, Investigation, Software, Writing – original draft, Writing – review & editing. **D. Lattuada:** Conceptualization, Data curation, Funding acquisition, Investigation, Supervision, Validation, Writing – original draft, Writing – review & editing.

Declaration of competing interest

The authors declare the following financial interests/personal relationships which may be considered as potential competing interests:

Irene Cetin reports financial support was provided by Italian Ministry of Health. Debora Lattuada has patent #WO2014173997A3 issued to Foundation IRCCS Ca' Granda Ospedale Maggiore Policlinico di Milano. If there are other authors, they declare that they have no known competing financial interests or personal relationships that could have appeared to influence the work reported in this paper.

Funding

This research was supported by the Italian Ministry of Health.

Availability of data and materials

The data that support the findings of this study are available from the corresponding author, [Danusso R.], upon reasonable request.

Supplementary materials

Supplementary material associated with this article can be found, in the online version, at doi:10.1016/j.chroma.2024.465614.

References

[1] J.C. Giddings, A. New, Separation concept based on a coupling of concentration and flow nonuniformities, Separat. Sci. 1 (1) (1966) 123–125, https://doi.org/10.1080/01496396608049439.
[2] C.L. Plavchak, W.C. Smith, C.R.M. Bria, S.K.R. Williams, New advances and applications in field-flow fractionation, Annu. Rev. Anal. Chem. 14 (1) (2021) 257–279, https://doi.org/10.1146/annurev-anchem-091520-052742. PMID: 33770457.
[3] D. Lattuada, B. Roda, C. Pignatari, R. Magni, F. Colombo, A. Cattaneo, A. Zattoni, I. Cetin, P. Reschiglian, G. Bolis, A tag-less method for direct isolation of human umbilical vein endothelial cells by gravitational field-flow fractionation, Anal. Bioanal. Chem. 405 (2–3) (2013) 977–984, https://doi.org/10.1007/s00216-012-6337-4. PMID: 22995996.
[4] S. Lee, D.Y. Kang, M. Park, P.S. Williams, Effect of carrier fluid viscosity on retention time and resolution in gravitational field-flow fractionation, Anal. Chem. 83 (9) (2011) 3343–3351, https://doi.org/10.1021/ac103002g. PMID: 21466170.
[5] P. Reschiglian, A. Zattoni, B. Roda, S. Casolari, M.H. Moon, J. Lee, J. Jung, K. Rodmalm, G. Cenacchi, Bacteria sorting by field-flow fractionation. Application to whole-cell Escherichia coli vaccine strains, Anal. Chem. 74 (19) (2002) 4895–4904, https://doi.org/10.1021/ac020199t. PMID: 12380810.
[6] GCh Lainioti, J. Kapolos, A. Koliadima, G. Karaiskakis, New separation methodologies for the distinction of the growth phases of Saccharomyces cerevisiae cell cycle, J. Chromatogr. A 1217 (11) (2010) 1813–1820, https://doi.org/10.1016/j.chroma.2010.01.042. PMID: 20117786.
[7] S. Guo, B.L. Qiu, C.Q. Zhu, Y.G. Yang, D. Wu, Q.H. Liang, N.Y. Han, Effects of comprehensive function of factors on retention behavior of microparticles in gravitational field-flow fractionation, J. Chromatogr. B Analyt. Technol. Biomed. Life Sci. 1031 (2016) 1–7, https://doi.org/10.1016/j.jchromb.2016.07.009. PMID: 27447927.
[8] R. Danusso, R. Rosati, L. Possenti, E. Lombardini, F. Gigli, M.L. Costantino, E. Ferrazzi, G. Casagrande, D. Lattuada, Human umbilical cord blood cells suffer major modification by fixatives and anticoagulants, Front. Physiol. 14 (2023) 1070474, https://doi.org/10.3389/fphys.2023.1070474. PMID: 37008002.
[9] P.S. Williams, T. Koch, Characterization of near-wall hydrodynamic lift forces using sedimentation field-flow - fractionation, Chem. Eng. Commun. 111 (1992) 121–147, https://doi.org/10.1080/00986449208935984, 1ISSN 15635201.
[10] M. Schimpf, K. Caldwell, J.C. Giddings, Field-Flow Fractionation Handbook, Chapter 1.4, p.72, John Wiley & Sons, 2000.
[11] E. Guetta, M.J. Simchen, K. Mammon-Daviko, D. Gordon, A. Aviram-Goldring, N. Rauchbach, G. Barkai, Analysis of fetal blood cells in the maternal circulation: challenges, ongoing efforts, and potential solutions, Stem. Cells Dev. 13 (1) (2004) 93–99, https://doi.org/10.1089/154732804773099290.
[12] S. Lee, J.C. Giddings, Experimental observation of steric transition phenomena in sedimentation field-flow fractionation, Anal. Chem. 60 (11) (1988) 2328–2333, https://doi.org/10.1021/ac00172a004.
[13] P.S. Williams, T. Koch, Characterization of near-wall hydrodynamic lift forces using sedimentation field-flow - fractionation, Chem. Eng. Commun. 111 (1992) 121–147, https://doi.org/10.1080/00986449208935984.
[14] R. Huang, T.A. Barber, M.A. Schmidt, R.G. Tompkins, M. Toner, D.W. Bianchi, R. Kapur, W.L. Flejter, A microfluidics approach for the isolation of nucleated red blood cells (nrbcs) from the peripheral blood of pregnant women, Prenat. Diagn. 28 (2008) 892–899, https://doi.org/10.1002/pd.2079.
[15] G.R. Nagy, Z. Bán, F. Sipos, A. Beke, C. Papp, Z. Papp, Isolation of epsilon haemoglobin-chain positive fetal cells with micromanipulation for prenatal diagnosis, Prenat. Diagn. 25 (2005) 398–402, https://doi.org/10.1002/pd.11.
[16] H.J. Sant, B.K. Gale, Geometric scaling effects on instrumental plate height in field flow fractionation, J. Chromatogr. A 1104 (2005) 282–290, https://doi.org/10.1016/j.chroma.2005.11.127.
[17] Janouskova J., Budinska M., Plockova J., and Chmelık J. Optimization of experimental conditions for the separation of small and large starch granules by gravitational field-flow fractionation, 2001. 914(1–2):183–7. doi:10.1016/s0021-9673(00)01090-6. PMID: 11358212.
[18] M.N. Myers, J.C. Giddings, Properties of the transition from normal to steric field-flow fractionation, Anal. Chem. 54 (13) (1982) 2284–2289, https://doi.org/10.1002/9780470027318.a2008.pub3.
[19] R. Polanowska-Grabowska, S. Raha, A.R. Gear, Adhesion efficiency, platelet density and size, Br. J. Haematol. 82 (4) (1992) 715–720, https://doi.org/10.1111/j.1365-2141.1992.tb06949.x. PMID: 1282829.
[20] M. Rosenfeld, Methylcellulose as a wetting agent in blood clot: in vivo studies, Blood 12 (4) (1957) 373–381. PMID: 13412766.
[21] A. Sekizawa, A. Farina, D. Kai, Z. Ji, Y. Wang, V.M. Falco, S. Elmes, D.W Bianchi, Improvement of fetal cell recovery from maternal blood: suitable density gradient for facs separation, Fetal Diagn. Ther. (1999), https://doi.org/10.1159/000020927. PMID: 10420047.
[22] R. Moreira, F. Chenlo, C. Silva, M. Torres, Rheological behaviour of aqueous methylcellulose systems: effect of concentration, temperature and presence of tragacanth, LWT-Food Sci. Technol. (84) (2017) 764–770, https://doi.org/10.1016/j.lwt.2017.06.050.
[23] B. Büyükurgancı, S.K. Basu, M. Neuner, J. Guck, A. Wierschem, F. Reichel, Shear rheology of methyl cellulose based solutions for cell mechanical measurements at high shear rates, Soft. Matter. 19 (9) (2023) 1739–1748, https://doi.org/10.1039/d2sm01515c. PMID: 36779239.